⌘ *Author's Choice*

THE JOURNAL OF BIOLOGICAL CHEMISTRY VOL. 288, NO. 5, pp. 3312–3321, February 1, 2013

Inositol Pyrophosphate Synthesis by Inositol Hexakisphosphate Kinase 1 Is Required for Homologous Recombination Repair*

Received for publication, June 29, 2012, and in revised form, December 12, 2012 Published, JBC Papers in Press, December 19, 2012, DOI 10.1074/jbc.M112.396556

Rathan S. Jadav[‡1], **Manasa V. L. Chanduri**[‡1], **Sagar Sengupta**[§2], **and Rashna Bhandari**[‡3]

From the [‡]*Laboratory of Cell Signalling, Centre for DNA Fingerprinting and Diagnostics, Hyderabad 500001 and the* [§]*National Institute of Immunology, Aruna Asaf Ali Marg, New Delhi 110067, India*

Background: DNA repair by homologous recombination (HR) is critical to maintain genomic integrity.
Results: Loss of inositol pyrophosphate synthesis by inositol hexakisphosphate kinase 1 (IP6K1) impairs HR in mammalian cells, leading to increased cell death.
Conclusion: We report a new player in mammalian HR repair.
Significance: As cancer chemotherapeutics act by causing DNA damage, IP6K1 inhibition may provide a novel route to supplement chemotherapy.

Inositol pyrophosphates, such as diphosphoinositol pentakisphosphate (IP_7), are water-soluble inositol phosphates that contain high energy diphosphate moieties on the inositol ring. Inositol hexakisphosphate kinase 1 (IP6K1) participates in inositol pyrophosphate synthesis, converting inositol hexakisphosphate (IP_6) to IP_7. In the present study, we show that mouse embryonic fibroblasts (MEFs) lacking IP6K1 exhibit impaired DNA damage repair via homologous recombination (HR). IP6K1 knock-out MEFs show decreased viability and reduced recovery after induction of DNA damage by the replication stress inducer, hydroxyurea, or the radiomimetic antibiotic, neocarzinostatin. Cells lacking IP6K1 arrest after genotoxic stress, and markers associated with DNA repair are recruited to DNA damage sites, indicating that HR repair is initiated in these cells. However, repair does not proceed to completion because these markers persist as nuclear foci long after drug removal. A fraction of IP6K1-deficient MEFs continues to proliferate despite the persistence of DNA damage, rendering the cells more susceptible to chromosomal aberrations. Expression of catalytically active but not inactive IP6K1 can restore the repair process in knock-out MEFs, implying that inositol pyrophosphates are required for HR-mediated repair. Our study therefore highlights inositol pyrophosphates as novel small molecule regulators of HR signaling in mammals.

Inositol pyrophosphates are water-soluble derivatives of inositol that contain pyrophosphate or diphosphate moieties in addition to monophosphates. The best characterized inositol pyrophosphates are IP_7 [4] (diphosphoinositol pentakisphosphate or PP-IP_5) and IP_8 (bisdiphosphoinositol tetrakisphosphate or $(PP)_2$-IP_4) (1–3). These energy-rich small molecules are present in all eukaryotic cells and are involved in a wide range of cellular functions including apoptosis, telomere length maintenance, osmoregulation, phosphate homeostasis, and insulin exocytosis. IP_7 and IP_8 are synthesized from inositol hexakisphosphate (IP_6) via two complementary pathways (3, 4). IP_6 kinases (IP6Ks) transfer a phosphate group from ATP to IP_6 to synthesize an isomer of IP_7 with a diphosphate moiety at the 5 position. 5-IP_7 is further phosphorylated by VIP1 to generate a second diphosphate at the 1 position, yielding IP_8 ($1,5(PP)_2$-IP_4) (5). In an alternate pathway, VIP1 generates 1-IP_7 from IP_6, which is then converted to IP_8 by IP6Ks. Mammals have three isoforms of IP_6 kinase, IP6K1, IP6K2, and IP6K3, whereas *Saccharomyces cerevisiae* have a single IP_6 kinase, KCS1 (6, 7).

Inositol pyrophosphates regulate protein function via two molecular mechanisms, protein binding and protein pyrophosphorylation (2, 3). A particular inositol pyrophosphate may selectively bind a protein and regulate its function. Examples include the specific binding of 1-IP_7 to PHO81, a cyclin-dependent kinase inhibitor that regulates phosphate homeostasis in

* This work was supported by the Wellcome Trust/Department of Biotechnology India Alliance (500020/Z/09/Z (to R. B.)) and core funds from the Centre for DNA Fingerprinting and Diagnostics, Hyderabad, India.
⌘ *Author's Choice*—Final version full access.
[1] Recipients of Junior and Senior Research Fellowships of the Council of Scientific and Industrial Research toward the pursuit of a Ph. D. degree of the Manipal University.
[2] Supported by National Institute of Immunology core funds; the Department of Biotechnology (DBT), India (Grant BT/PR11258/BRB/10/645/2008); the Department of Science and Technology (DST), India (Grant SR/SO/BB-08/2010); the Indo-French Centre for the Promotion of Advanced Research (IFCPAR) (Grant IFC/4603-A/2011/1250); and the Council of Scientific and Industrial Research (CSIR), India (Grant 37(1541)/12/EMR-II).
[3] Supported by a Senior Fellowship from the Wellcome Trust/DBT India Alliance (500020/Z/09/Z); and the DBT Innovative Young Biotechnologist Award (Grant BT/BI/12/045/2008). To whom correspondence should be addressed: Laboratory of Cell Signalling, Centre for DNA Fingerprinting and Diagnostics, Bldg. 7 Gurhakalpa, 5-4-399/B Nampally, Hyderabad 500001, India. Tel.: 91-40-24749430; Fax: 91-40-24749448; E-mail: rashna@cdfd.org.in.

[4] The abbreviations used are: IP_7, diphosphoinositol pentakisphosphate; IP_4, inositol tetrakisphosphate; IP_5, inositol pentakisphosphate; IP_6, inositol hexakisphosphate; IP_8, bisdiphosphoinositol tetrakisphosphate; IP6K, inositol hexakisphosphate kinase; HR, homologous recombination; HU, hydroxyurea; NCS, neocarzinostatin; MEF, mouse embryonic fibroblast; DSB, double-strand break; MTT, (3-(4,5-dimethylthiazol-2-yl)-2,5-diphenyltetrazolium bromide; TUNEL, terminal deoxynucleotidyltransferase-mediated dUTP nick end-labeling; EdU, 5-ethynyl-2′-deoxyuridine; PI, propidium iodide; BLM, Bloom syndrome protein; VSV, vesicular stomatitis virus; γH2AX, phosphorylated histone H2AX.

yeast (8), and 5-IP_7 binding to the pleckstrin homology domain of Akt (9, 10). Any inositol pyrophosphate may act as a phosphate donor in the presence of divalent metal ions, transferring its β-phosphate to a prephosphorylated serine residue to form pyrophosphoserine (11, 12). Recent studies have revealed that IP_7-mediated protein pyrophosphorylation regulates vesicle trafficking in mammals and glycolysis in yeast (13, 14).

IP_6 kinases have been shown to be involved in the maintenance of genomic integrity in yeast. *S. cerevisiae* strains lacking KCS1 have longer telomeres than wild type strains (15, 16), and inositol pyrophosphates support DNA hyperrecombination in yeast containing a mutant form of protein kinase C (17, 18). Genomic insults that occur in mitotic cells due to stalled or collapsed replication forks or exposure to DNA damage agents (19) induce DNA double-strand breaks (DSBs) and trigger repair via homologous recombination (HR). A complex cell signaling cascade coordinates DNA repair with progression through cell cycle checkpoints (20). Mitotic cells with impaired HR may stop dividing and undergo cell death or may overcome cell cycle checkpoints and accumulate mutations in their DNA, leading to cancer.

In the HR signaling network, we now report a new player, IP6K1. Here, we examine DNA damage repair in mouse embryonic fibroblasts (MEFs) derived from IP6K1 knock-out mice. Our data reveal that inositol pyrophosphates synthesized by IP6K1 are essential for HR-mediated DNA repair. We observe that MEFs lacking IP6K1 can initiate HR but fail to complete the process, resulting in cell death or accumulation of chromosomal aberrations. IP6K1 is therefore required to protect genomic integrity in mammalian cells.

EXPERIMENTAL PROCEDURES

Cell Lines—Single cell-derived wild type ($IP6K1^{+/+}$) and IP6K1 knock-out ($IP6K1^{-/-}$) MEF cell lines were generated from $IP6K1^{+/+}$ and $IP6K1^{-/-}$ embryo-derived immortalized fibroblasts (21) by dilution plating. A catalytically inactive form of mouse IP6K1 (K226A/S334A) was generated by site-directed mutagenesis. $IP6K1^{-/-}$ MEFs expressing active or inactive forms of IP6K1 were generated by retroviral transduction. cDNA encoding Myc-tagged active and inactive IP6K1 were cloned into pCX4Neo plasmid (22) and co-transfected with VSV-G- and VSV-GP-encoding plasmids into PlatE cells (Cell Biolabs) using PolyFect reagent (Qiagen). Retroviral particles derived from these cells were used to infect $IP6K1^{-/-}$ MEFs, and following selection in G418 (400 μg/ml) for 7 days, single cell-derived lines were generated by dilution plating. Cell lines were maintained in complete DMEM (HyClone) supplemented with 10% (v/v) fetal bovine serum (FBS, Invitrogen), Pen-Strep (100 μg/ml streptomycin, 100 units/ml penicillin; Invitrogen), with or without G418 (200 μg/ml). Cells were grown at 37 °C in an incubator containing 5% CO_2.

Antibodies and Reagents—Primary antibodies for immunofluorescence, Western blot, and FACS analyses were obtained from the following sources: rabbit anti-BLM (A310-167A, Bethyl Laboratories); DR1034, (Calbiochem); rabbit anti-Rad51 (PC130, Calbiochem); rabbit anti-γH2AX (ab2893, Abcam); rabbit anti-H3S10 (ab5176, Abcam); rabbit anti-IP6K1 (HPA040825, Sigma-Aldrich); and mouse anti-GAPDH (G8795, Sigma-Aldrich). DNA-damaging agents used for this study were obtained from the following sources: hydroxyurea (HU, H8627, Sigma-Aldrich); neocarzinostatin (NCS, N9162, Sigma-Aldrich); and mitomycin C (M0503, Sigma-Aldrich). All other reagents, unless otherwise stated, were procured from Sigma-Aldrich.

Cell Survival Assay—MEFs were seeded in 24-well plates at a density of 30,000 cells/well and allowed to grow overnight. Cells were treated with HU or NCS at the indicated concentrations for 12 h, spent medium containing drug was removed, and cells were washed with PBS. Cells were then incubated for different lengths of time in normal medium to allow them to recover from genotoxic stress. Cell viability was analyzed by MTT assay at each time point. Absorbance values at 570 nm were determined using a microplate reader (BioTek Instruments). Cell survival was expressed as a -fold change in cell population over viable cells present immediately after drug treatment for 12 h. Data were analyzed using GraphPad Prism 5.

Cell Cycle Analysis—Cells were grown in 35-mm dishes at a density of 2×10^5 cells/dish. At 60% confluence, cells were treated with HU or NCS for 12 h. After treatment, medium containing drug was removed, and normal medium was added for recovery of the cells from genotoxic stress for different lengths of time. Cells were fixed in 70% ethanol overnight at −20 °C and stained with propidium iodide (PI; 20 μg/ml in PBS containing 0.1% Triton X-100 and 0.2 mg/ml RNase A) for 30 min at 37 °C. Alternatively, 5-ethynyl-2′-deoxyuridine (EdU) labeling and cell cycle analysis were conducted using the Click-iT cell proliferation assay kit (C35002, Invitrogen), as per the manufacturer's instructions. Cells were analyzed by flow cytometry (FACSAria, BD Biosciences). Data analysis to determine the stages of the cell cycle was performed using FlowJo (for PI-labeled cells) or FACSDiva (BD Biosciences; for EdU-labeled cells), and results were plotted using GraphPad Prism 5.

Cell Viability Assay by PI Staining—MEFs were treated with HU for 12 h and allowed to recover for different lengths of time. Cells were harvested, washed with PBS, and stained with PI (2 μg/ml in PBS) for 2 min at room temperature. Under these conditions, live cells exclude dye, and only nonviable cells are stained. Live *versus* dead cells were analyzed by flow cytometry (Accuri C6, BD Biosciences).

Immunofluorescence—Localization of the DNA damage response proteins, phosphorylated histone H2AX (γH2AX), RAD51, and BLM, and the mitotic marker, H3S10 (histone H3 phosphorylated on Ser-10) upon genotoxic stress was analyzed by immunofluorescence following hypotonic lysis. Briefly, cells were seeded on coverslips in 12-well plates at a cell density of 30,000–40,000 cells/well and incubated overnight. Cells were treated with HU or NCS for 12 h, and immunofluorescence was carried out as described earlier (23). Images were acquired by confocal fluorescence microscopy (Zeiss LSM 510 META). Nuclear foci were visualized using LSM Browser software, by linearly changing the contrast uniformly across all images, for background correction. 70–100 cells were analyzed per experiment to count nuclear foci.

TUNEL Assay—MEFs were seeded in 35-mm dishes at a density of 2×10^5 cells/dish. At 60% confluence, cells were treated with HU for 12 h and allowed to recover for different lengths of

time. Cells were harvested and fixed in 70% ice-cold ethanol overnight at −20 °C. TUNEL assay to detect DNA damage was conducted using an APO-BrdU TUNEL assay kit (A35127, Invitrogen), as per the manufacturer's instructions. Cells were analyzed by flow cytometry (FACSAria, BD Biosciences). Viable cells were analyzed for the presence of DNA damage by excluding the hypodiploid (sub-G_0/G_1) population, using the FACSDiva software (BD Biosciences). Median fluorescence values of the treated cells were plotted as a -fold difference over untreated controls, using GraphPad Prism 5.

Cytogenetic Analysis—MEFs were treated with mitomycin C (300 nM) for 12 h, washed, and treated with colcemid (0.1 μg/ml) for 4 h. Cells were harvested, subjected to hypotonic swelling in prewarmed 0.075 M KCl for 15 min at 37 °C, and fixed in three changes of 3:1 methanol/glacial acetic acid at room temperature for 10 min each. Cells resuspended in fixative were dropped onto humidified, clean, and chilled glass slides. Slides were dried and stained with 3% Giemsa in phosphate buffer (pH 6.8). Individual metaphase spreads were analyzed using bright field microscopy (Zeiss Axio Scope) and photographed, and structural chromosomal aberrations (chromatid breaks and triradial and quadriradial chromosomes) were scored manually.

IP6K2 Knockdown by shRNA—Plasmids encoding either a nontargeting shRNA (Sigma-Aldrich SHC016) or shRNA directed against mouse IP6K2 (Sigma-Aldrich, TRCN0000202175 or TRCN0000202065) were co-transfected with VSV-G- and VSV-GP-encoding plasmids into the Phoenix amphotropic packaging cell line, using PolyFect reagent (Qiagen), and incubated at 37 °C and 5% CO_2 for virion formation. After 48 h, supernatant was collected and filtered through a 0.45-μm syringe filter unit. Lentiviral particles carrying either nontargeting shRNA or both IP6K2-directed shRNA constructs were used to infect MEFs for 48 h. At the 36th h, cells were treated with HU for 12 h followed by recovery for 6 h, and immunofluorescence was carried out as described above. Immunoblotting with an IP6K antibody in IP6K1$^{-/-}$ MEFs revealed a 40% knockdown of IP6K2 expression in cells transduced with IP6K2-targeting shRNA when compared with nontargeting shRNA (data not shown).

RESULTS

Reduced Viability of IP6K1 Knock-out MEFs after Induction of DSBs—Treatment with hydroxyurea (HU), a ribonucleotide reductase inhibitor, leads to replication stress and arrests cells at the G_1/S boundary of the cell cycle (24). Prolonged replication stalling by HU treatment generates one-ended DSBs and initiates DNA repair via HR. The radiomimetic antibiotic NCS directly causes double-strand breaks in DNA, triggering HR-mediated repair (19). MEFs derived from IP6K1 knock-out embryos and their wild type litter mates have been used to examine the cellular functions of IP6K1 (9, 13, 14, 21). IP6K1$^{+/+}$ and IP6K1$^{-/-}$ MEFs were treated with a sublethal dose of HU or NCS for 12 h, and cell viability was determined after a recovery period of 24 h. IP6K1$^{-/-}$ cells display a more pronounced drop in viability after HU removal when compared with IP6K1$^{+/+}$ MEFs (Fig. 1*A*). After recovery from NCS treatment, both IP6K1$^{+/+}$ and IP6K1$^{-/-}$ MEFs proliferate, but the extent of proliferation is lower in knock-out MEFs (Fig. 1*B*).

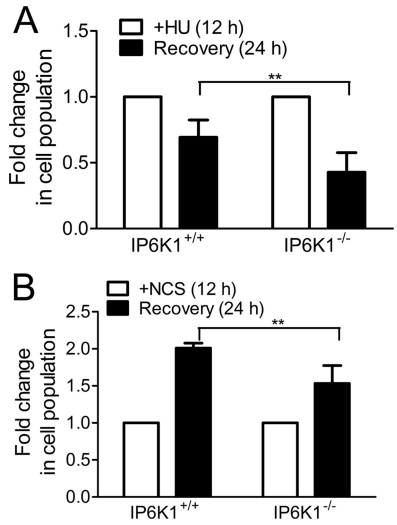

FIGURE 1. **Impaired recovery of IP6K1$^{-/-}$ MEFs following DNA damage.** *A* and *B*, cell viability measurement by MTT assay following treatment with HU (0.5 mM) (*A*) or NCS (0.25 μg/ml) (*B*) for 12 h and recovery after drug removal for 24 h. Data are mean ± S.E. from three independent experiments. *p* values are from a two-tailed Student's *t* test (**, $p \leq 0.01$).

To monitor cell cycle progression of MEFs subjected to genotoxic stress, we used flow cytometry analysis to measure the extent of arrest and release during a 12-h period after drug removal. IP6K1$^{-/-}$ cells arrest at the G_1/S boundary to the same extent as IP6K1$^{+/+}$ cells, indicating that checkpoint activation subsequent to DNA damage is intact in the absence of IP6K1 (Fig. 2*A*). However, fewer IP6K1$^{-/-}$ cells enter the S phase after HU removal, suggesting their inability to recover from DNA damage (Fig. 2, *A* and *B*). Conversely, a higher number of knock-out MEFs are present in the hypodiploid (sub-G_0/G_1) population after a 12-h recovery period (Fig. 2, *A* and *C*). We confirmed that this population represents nonviable cells by measuring propidium iodide uptake following HU treatment and recovery (Fig. 2*D*). Upon treatment with NCS, IP6K1$^{+/+}$ and IP6K1$^{-/-}$ MEFs arrest similarly at the G_2/M boundary (Fig. 2*E*). However, a lower fraction of IP6K1$^{-/-}$ MEFs recovers from the arrest and is present in the G_0/G_1 phase 12 and 24 h after drug removal (Fig. 2*F*), and there is a concomitant increase in the number of hypodiploid IP6K1$^{-/-}$ cells (Fig. 2*G*). Together, these data reveal that subsequent to DNA damage, IP6K1 knock-out cells show reduced recovery and increased cell death when compared with wild type cells.

HR Is Initiated but Stalls in IP6K1 Knock-out MEFs—Loss of cell viability during recovery from genotoxic stress may be attributed to a defect in DNA repair. The DNA damage response may be monitored by the recruitment of DNA repair markers to the site of damage. An early event following HU-induced replication stress is the accumulation of γH2AX at the site of DNA damage (25), and the clearance of nuclear γH2AX foci reflects successful DNA repair. We monitored nuclear γH2AX levels in MEFs immediately after HU treatment and 6 h after drug removal, the time at which S phase entry in wild type MEFs is maximal, and DNA damage is expected to be repaired. IP6K1$^{-/-}$ MEFs display a significantly higher number of γH2AX foci following HU treatment (Fig. 3, *A* and *B*). This may reflect accumulation of greater DNA damage in knock-out

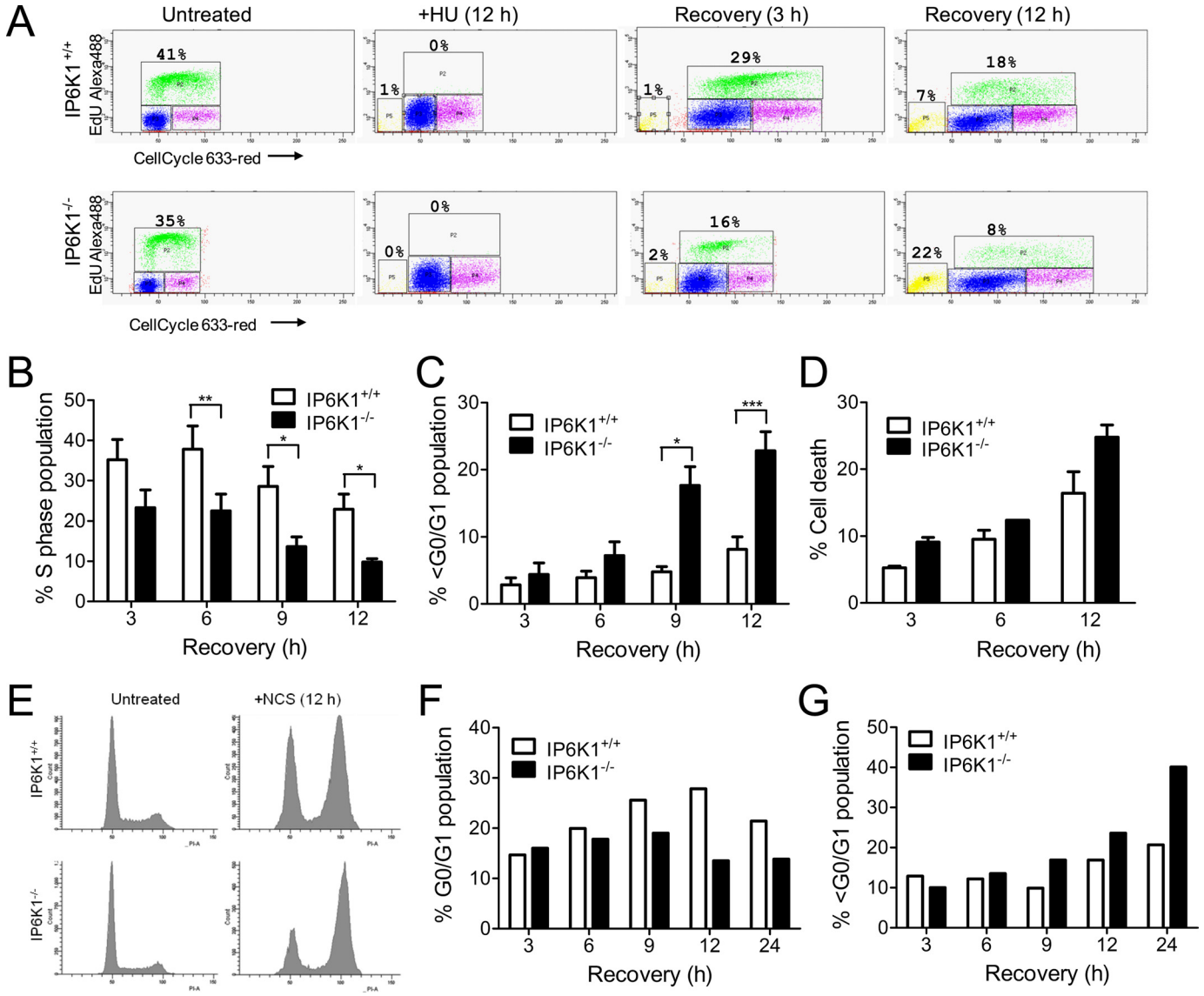

FIGURE 2. **Cell cycle progression of MEFs in response to DNA damage.** *A*, cell cycle profiles of MEFs following HU (0.2 mM) treatment and recovery for the indicated times. Dot plots representative of three independent experiments show DNA content on the *x* axis against EdU incorporation on the *y* axis; *boxes* mark cells in the sub-G_0/G_1 (*yellow*), G_0/G_1 (*blue*), S (*green*), and G_2/M (*magenta*) phases of the cell cycle. Percentages of cells present in sub-G_0/G_1 and S populations are indicated. *Alexa488*, Alexa Fluor 488. *B* and *C*, cell cycle analysis to monitor recovery at the indicated times after HU (0.2 mM) treatment by measuring entry into S phase (*B*) and cell death (sub-G_0/G_1 ($<G_0/G_1$) population) (*C*). Data are mean ± S.E. from four independent experiments. *D*, cell viability assay by PI staining of MEFs following HU (0.2 mM) treatment and recovery for the indicated times. Dead cells stained with PI are expressed as a percentage of total cell count. Data are mean ± range from two independent experiments. *E*, flow cytometry analysis of PI-stained MEFs prior to or after NCS (0.25 μg/ml) treatment. Histograms indicate a normal cell cycle profile in untreated cells, and arrest at the G_2/M boundary in NCS-treated cells. Data are representative of three independent experiments. *F* and *G*, cell cycle analysis to monitor recovery at the indicated times after NCS (0.25 μg/ml) treatment by measuring entry into the G_0/G_1 phase (*F*) and cell death (sub-G_0/G_1 population) (*G*). Data are representative of three independent experiments. *p* values are from a two-tailed Student's *t* test (*, $p \leq 0.05$, **, $p \leq 0.01$, ***, $p \leq 0.001$).

MEFs during the period of drug treatment. Although γH2AX foci are nearly undetectable in IP6K1$^{+/+}$ MEFs after recovery from HU treatment, indicating repair of damaged DNA, they continue to persist at high levels in IP6K1$^{-/-}$ MEFs, suggesting that these cells have defective or delayed DNA damage repair.

RAD51 is recruited to the sites of DSBs in a γH2AX-dependent process and participates in the early steps of HR, homology search and strand invasion (26). BLM is a RecQ family helicase that participates in DNA damage sensing at an early stage and in Holliday junction resolution toward the end of HR (27). We used these proteins as surrogate markers to track initiation and completion of HR in HU-treated MEFs. As with γH2AX, more RAD51 and BLM foci are observed in IP6K1$^{-/-}$ MEFs immediately after HU treatment (Fig. 3, *C–F*). These foci persist 6 h after HU removal in knock-out, but not in wild type MEFs. Interestingly, we observed a variation in the average number of foci marked by γH2AX, RAD51, and BLM antibodies after a 12-h HU treatment of wild type MEFs. This could reflect a difference in sensitivity between these antibodies or a difference in the temporal association of the respective proteins at the sites of damage. We also noted experimental variation in foci counts using the same antibody, but the trend of persistent DNA damage markers in IP6K1$^{-/-}$ MEFs was conserved throughout. Upon treatment with NCS, BLM accumulation is

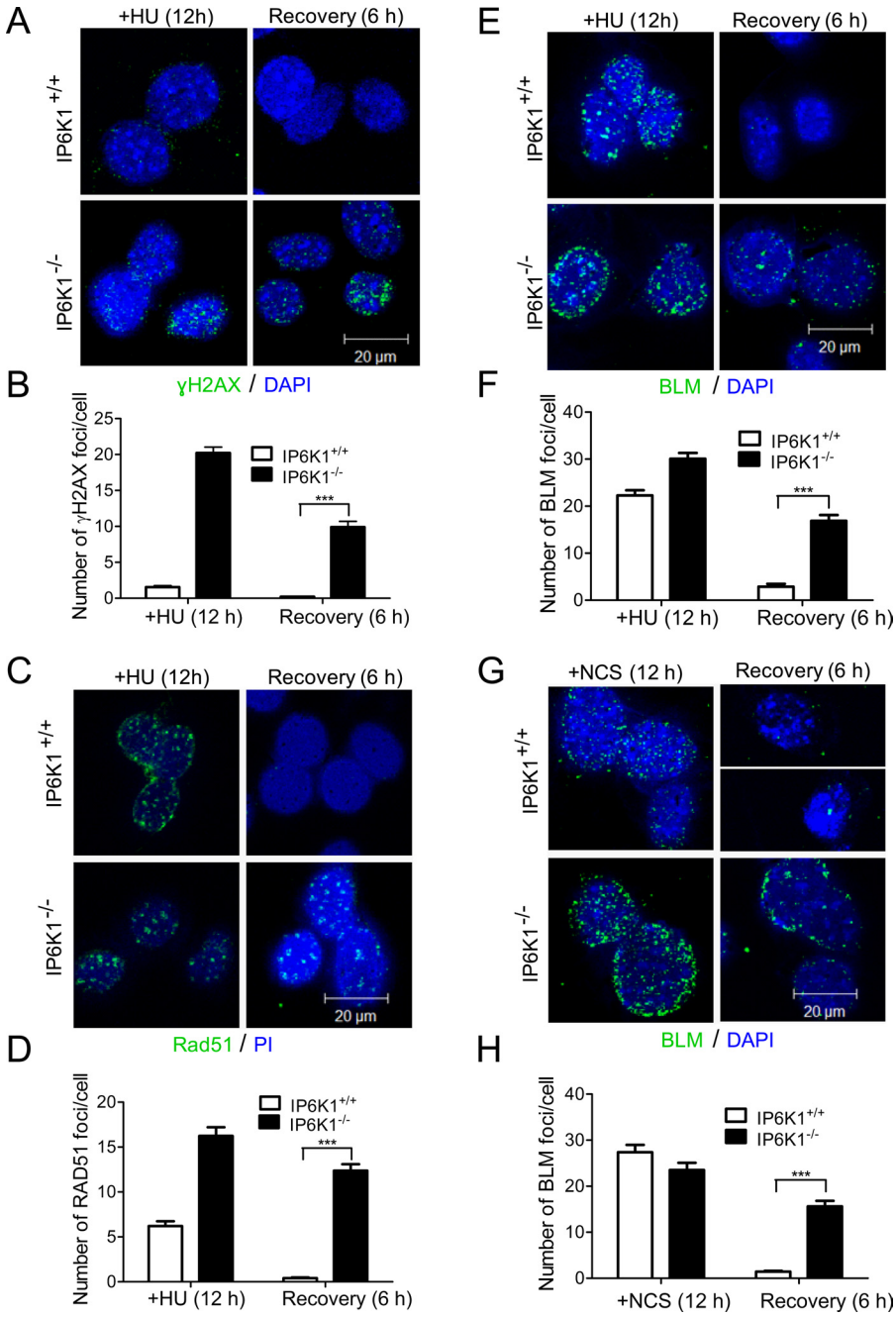

FIGURE 3. **Recruitment of HR markers following DNA damage.** Immunofluorescence of DNA repair markers in nuclei of MEFs after drug treatment and recovery for the indicated times was measured. *A*, γH2AX foci after HU (0.5 mM) treatment. *B*, quantitation of *A*; data (mean ± S.E. $n = 150$) are representative of two experiments. *C*, RAD51 foci after HU (0.5 mM) treatment. *D*, quantitation of *C*; data (mean ± S.E. $n = 130$) are representative of two experiments. *E*, BLM foci after HU (0.5 mM) treatment. *F*, quantitation of *E*; data (mean ± S.E. $n = 80$) are representative of two experiments. *G*, BLM foci after NCS (0.25 μg/ml) treatment. *H*, quantitation of *G*; (mean ± S.E. $n = 70$). Images compiled from different regions of a single micrograph are juxtaposed where required and separated by a *white line*. *p* values are from a two-tailed Student's *t* test (***, $p \leq 0.001$).

similar in IP6K1$^{+/+}$ and IP6K1$^{-/-}$ MEFs, but after recovery, BLM foci persist in knock-out cells and are back to base-line levels in wild type cells (Fig. 3, *G* and *H*). Thus far, our data indicate that the process of DNA repair via HR is successfully initiated in the absence of IP6K1, but cannot be completed, leading to increased cell death.

IP6K1 Loss Increases Chromosomal Damage Susceptibility—We wondered whether the persistence of RAD51 and BLM foci in IP6K1$^{-/-}$ cells 6 h after recovery from HU treatment reflects the absence of HR-mediated DNA repair or whether repair is delayed, but eventually complete. We therefore examined MEFs treated with HU for nuclear BLM foci at longer time periods of recovery. A high number of BLM foci continue to persist 8 and 10 h following HU removal in IP6K1$^{-/-}$ MEFs (Fig. 4, *A* and *B*). Persistence of BLM foci may be indicative of defective DNA repair, but could also reflect incomplete dissolution of DNA repair complexes despite the completion of HR. We therefore monitored DNA repair subsequent to HU removal by conducting a TUNEL assay to measure DNA damage. Although the level of TUNEL staining falls down to the

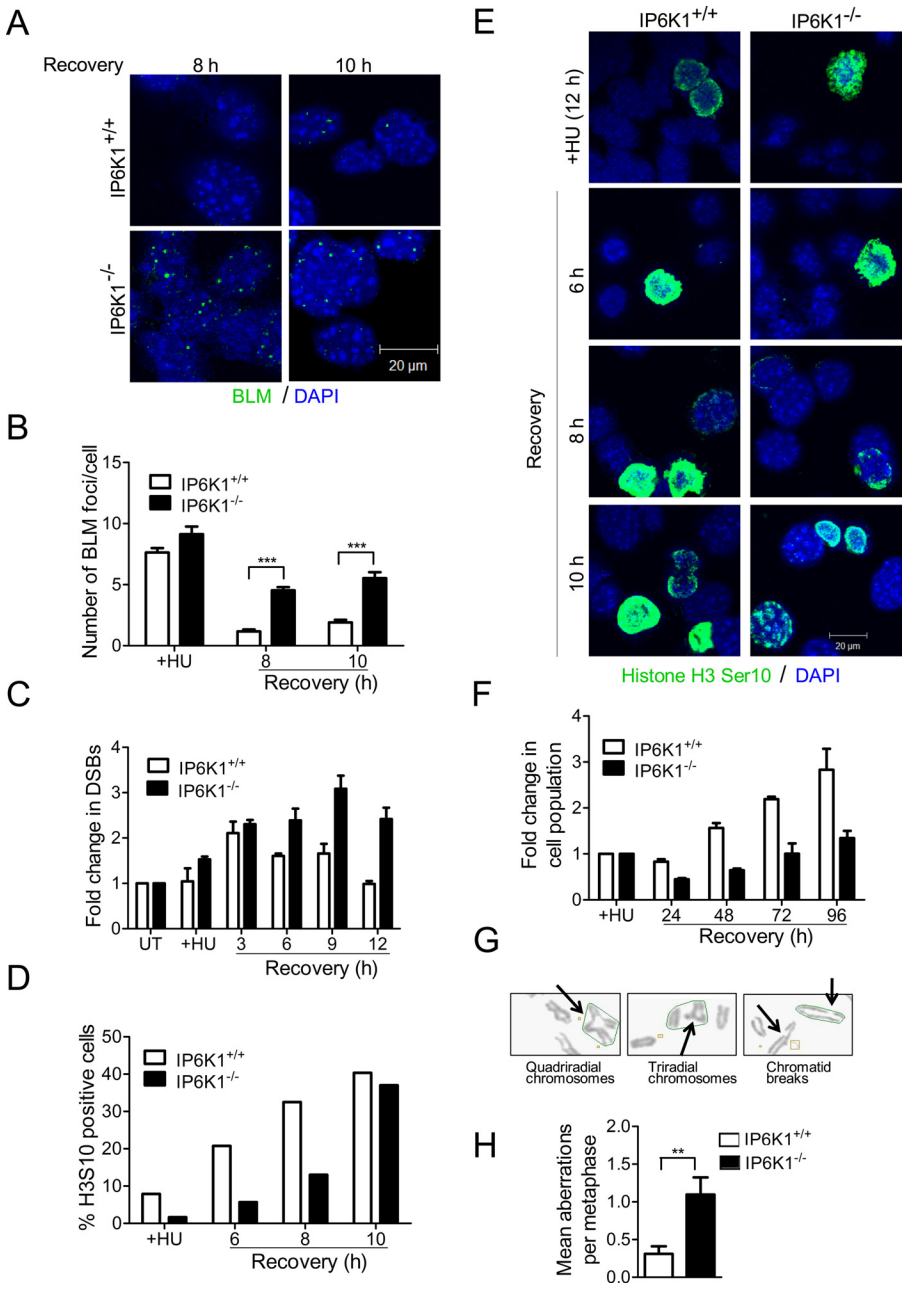

FIGURE 4. **Persistence of DNA damage in IP6K1 knock-out MEFs.** *A*, BLM foci formation in nuclei after HU (12 h, 0.5 mM) treatment of MEFs and recovery for the indicated times. *B*, quantitation of *A*; data (mean ± S.E. $n = 100$) are representative of two experiments. *C*, detection of DNA DSBs by TUNEL staining and flow cytometry analysis after HU (12 h, 0.5 mM) treatment of MEFs and recovery for the indicated times; bars represent mean ± range of two independent experiments. *D*, quantitation of histone H3 Ser-10 phosphorylation in MEFs after HU (12 h, 0.5 mM) treatment and recovery for the indicated times; bars indicate the percentage of positive cells ($n = 140$; representative of two experiments). *E*, representative immunofluorescence images for *D*. *F*, cell viability measurement by MTT assay following treatment with HU (12 h, 0.5 mM) and recovery for the indicated times; bars represent mean ± range of two independent experiments. *G*, representative images showing chromosomal lesions (marked by *arrows*) found in metaphase spreads from MEFs treated with mitomycin C (12 h, 300 nM). *H*, quantitation of *G*; data (mean ± S.E. $n = 41$) are representative of two experiments. *p* values are from a two-tailed Student's *t* test (**, $p \leq 0.01$, ***, $p \leq 0.001$).

base-line 12 h after drug removal in IP6K1$^{+/+}$ MEFs, DNA damage continues to persist in IP6K1$^{-/-}$ MEFs (Fig. 4*C*). Increased cell death at 9 and 12 h after HU removal in IP6K1$^{-/-}$ MEFs (Fig. 2, *C* and *D*) is thus attributable to the persistence of DNA damage in these cells.

To determine whether IP6K1$^{-/-}$ MEFs cross the G_2/M checkpoint and enter mitosis despite the persistence of damaged DNA, we stained cells for the presence of histone H3 phosphorylation at Ser-10, a marker for the initiation of mitosis (28). An increase in the mitotic population in IP6K1$^{+/+}$ MEFs follows the timeline of DNA repair (Fig. 4, *D* and *E*). IP6K1 knock-out MEFs display delayed entry into mitosis 10 h after HU removal (Fig. 4*D*) despite the persistence of DNA damage (Fig. 4*C*). Indeed, when proliferation of MEFs is monitored up to 4 days after HU removal, there is an eventual increase in viable IP6K1$^{-/-}$ MEFs, although it is still lower than IP6K1$^{+/+}$ MEFs (Fig. 4*F*). Proliferation of cells by continuing DNA replication without repairing DNA damage can result in the accumulation of chromosomal lesions (29). Defects in HR can lead to increased sensitivity to mitomycin C, a drug that induces DNA

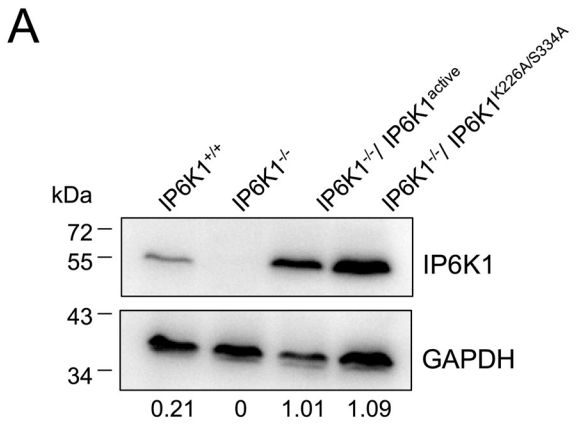

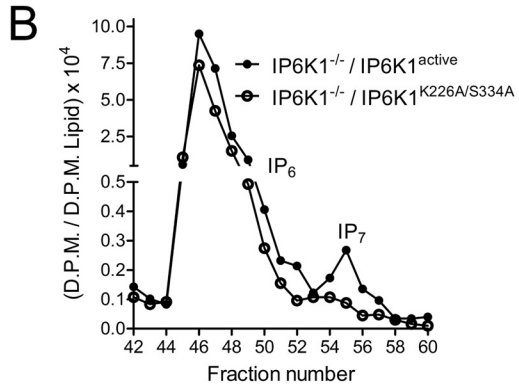

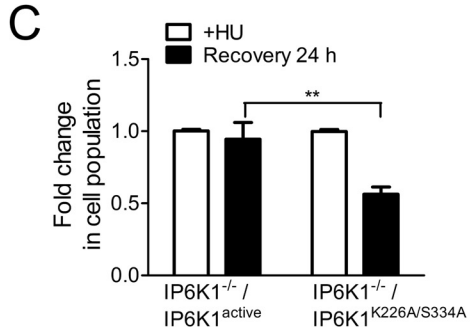

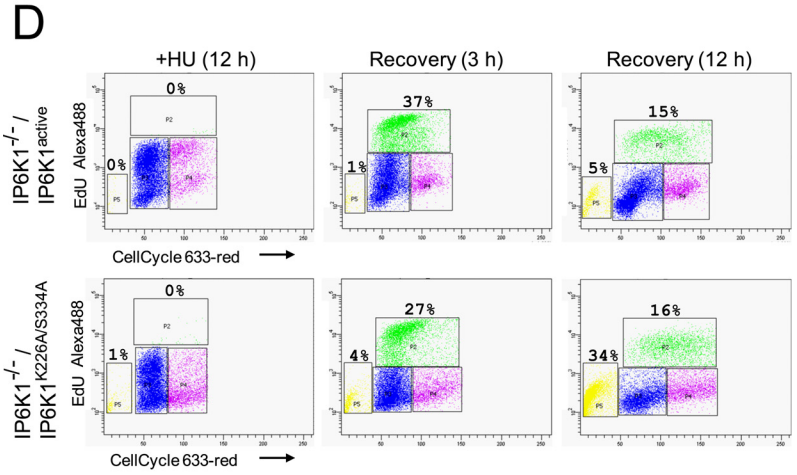

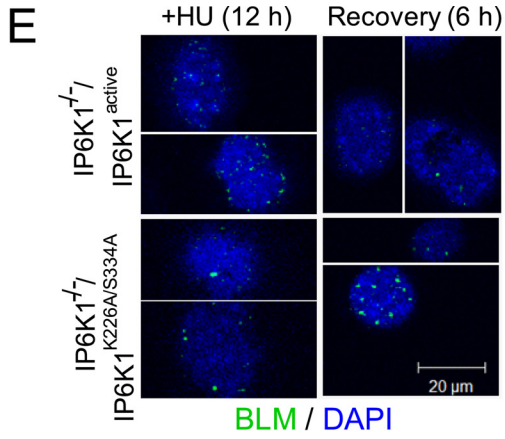

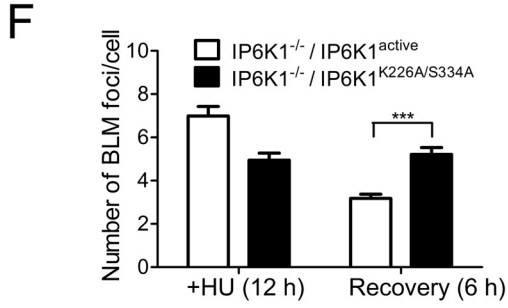

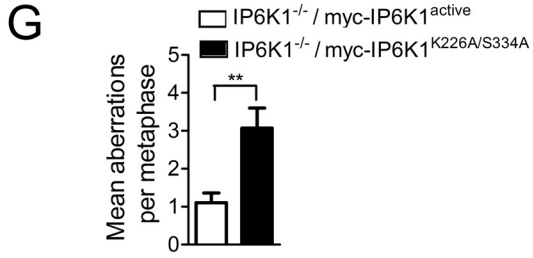

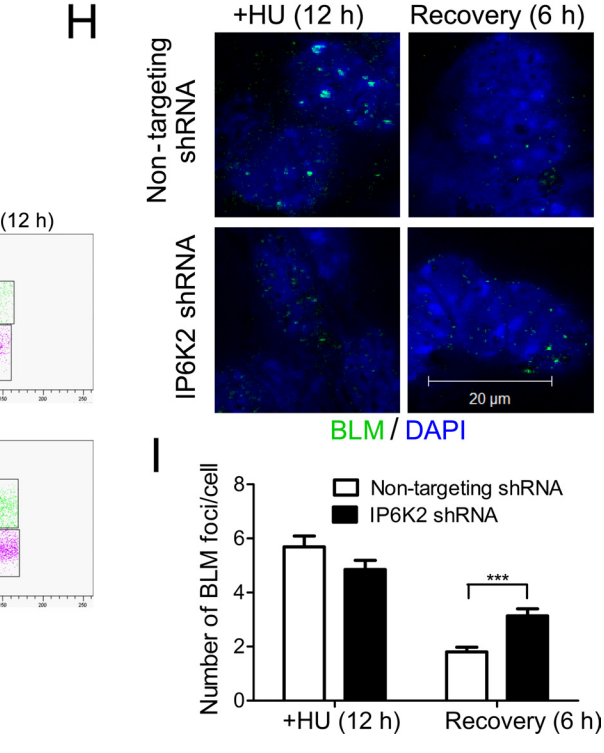

interstrand cross-links, blocking DNA replication (19). Analysis of metaphase spreads following mitomycin C treatment may therefore be used to probe defects in DNA repair (30). When treated with mitomycin C, IP6K1$^{-/-}$ MEFs show more chromosomal abnormalities, such as triradial and quadriradial chromosomes and chromatid breaks, when compared with IP6K1$^{+/+}$ MEFs (Fig. 4, *G* and *H*).

Inositol Pyrophosphate Synthesis Is Required for HR-mediated DNA Repair—Although the primary role of IP_6 kinases is the synthesis of inositol pyrophosphates, these enzymes are also known to regulate cell function independent of their catalytic activity (31). To determine whether the role of IP6K1 in HR is dependent upon its inositol pyrophosphate synthesis activity, we stably expressed active and catalytically inactive forms of IP6K1 in IP6K1$^{-/-}$ MEFs (Fig. 5*A*). IP6K1$^{-/-}$ MEFs expressing active IP6K1 displayed higher levels of IP_7 when compared with their counterparts that express inactive IP6K1 (Fig. 5*B*). Cell viability after recovery from HU treatment was restored by expressing active IP6K1 in IP6K1$^{-/-}$ MEFs, but cells expressing inactive IP6K1 show reduced viability, mimicking the phenotype of parent IP6K1$^{-/-}$ cells (Fig. 5*C*). A similar phenomenon was observed on analysis of cell cycle progression following HU treatment. IP6K1$^{-/-}$ cells expressing active IP6K1 enter the S phase and recover from HU treatment, whereas cells expressing inactive IP6K1 demonstrate reduced entry into S phase and a higher population of hypodiploid cells (Fig. 5*D*). HR repair after HU treatment was examined in these cells by monitoring BLM foci accumulation in nuclei (Fig. 5, *E* and *F*). BLM foci persist after recovery from HU treatment in cells expressing inactive IP6K1, but the foci are reduced in cells expressing active IP6K1. When treated with mitomycin C, IP6K1$^{-/-}$ MEFs expressing inactive IP6K1 accumulate a higher number of chromosomal abnormalities when compared with MEFs expressing active IP6K1 (Fig. 5*G*). Taken together, these data strongly indicate that inositol pyrophosphate synthesis by IP6K1 is essential for HR-mediated repair of damaged DNA.

Most mammalian cells are known to express two isoforms of IP_6 kinase, IP6K1 and IP6K2. IP6K1 knock-out MEFs display an ~70% reduction in IP_7 levels (21), and IP6K2 knock-out MEFs reduce IP_7 by 38% (32), implying that IP_7 production in MEFs is dependent on both IP_6 kinase isoforms. We wondered whether the marginal levels of repair observed in IP6K1$^{-/-}$ MEFs following HU treatment are due to IP_7 production by IP6K2. Although wild type MEFs expressing a nontargeting shRNA show recovery from HU treatment, MEFs targeted with IP6K2-specific shRNA display reduced recovery, as reflected by persistent nuclear staining with BLM (Fig. 5, *H* and *I*). These data suggest that there is some redundancy in the function of IP6K1 and IP6K2 with regard to the synthesis of IP_7 involved in HR-mediated DNA repair. Expression of a nontargeting control shRNA in IP6K1$^{-/-}$ MEFs abolished any recovery following HU treatment (data not shown), perhaps due to the added stress of viral transduction coupled with DNA damage, making it difficult to interpret the effects of simultaneously reducing IP6K1 and IP6K2 on DNA repair.

DISCUSSION

Our study identifies IP6K1 as a key player in HR-mediated DNA repair. Specifically, we have shown that cells lacking IP6K1 are able to initiate HR after being subjected to genotoxic stress, but fail to repair damaged DNA. As a result, many IP6K1 knock-out cells undergo death, and those that survive accumulate chromosomal lesions. Functional down-regulation of many proteins involved in HR leads to reduced recruitment of the HR marker RAD51 to the sites of DNA damage (33, 34). In contrast, IP6K1 knock-out cells accumulate a higher number of γH2AX and RAD51 foci, which may reflect greater DNA damage, but nonetheless indicate that HR initiation is normal in these cells. Therefore, IP6K1 is a rare factor required for downstream processes during HR, such as strand exchange, DNA synthesis, and Holliday junction resolution.

Our results may be examined in the context of the reported pro-recombinogenic effect of the yeast IP_6 kinase, KCS1 (17, 18). *kcs1*Δ yeast show reduced survival after treatment with phleomycin, which causes DNA DSBs (35). Although yeast have a single IP_6 kinase, mammals express three IP6K isoforms. IP6K3 is expressed primarily in the brain and not found in most peripheral tissues (7). Although IP6K1 and IP6K2 are expressed in most cells and tissues, they have been shown to participate in nonoverlapping cellular functions. For example, insulin release in pancreatic β cells is dependent on IP_7 synthesis by IP6K1 (36), whereas IP6K2 is a key pro-apoptotic regulator, even in cell types that possess both isoforms (37). Mouse knock-out models for these enzymes also display divergent phenotypes. IP6K1 knock-out male mice are infertile, lacking mature spermatozoa, and have reduced serum insulin levels (21), whereas IP6K2 knock-out males are fertile and display normal serum insulin (32). When challenged with an oral carcinogen, IP6K2 knock-out mice developed aerodigestive tract tumors (32). This phenotype was attributed to a critical role for IP6K2 in apoptosis. The functional redundancy, if any, between IP6K1 and IP6K2 in the context of the whole organism is not clear. Therefore, challenging IP6K1 knock-out mice with a carcinogen may clarify whether IP6K1 and IP6K2 play redundant or nonover-

FIGURE 5. **Inositol pyrophosphate synthesis by IP6K1 is required for DNA repair.** *A*, immunoblotting of cell extracts from MEFs of indicated genotypes, with IP6K1 and GAPDH antibodies. *B*, IP_6 and IP_7 levels in IP6K1$^{-/-}$ MEFs rescued with active and inactive forms of IP6K1 was measured by [^{3}H]inositol labeling as described previously (21). Soluble inositol phosphate counts were normalized to total lipid inositol count and plotted using GraphPad Prism 5. *C*, cell viability measurement by MTT assay after treatment of MEFs with HU (12 h, 0.5 mM) and recovery for the indicated times. Data are mean ± S.E. from three independent experiments. *D*, cell cycle profiles of MEFs following HU (0.2 mM) treatment and recovery for the indicated times. Dot plots representative of two independent experiments show DNA content on the *x* axis against EdU incorporation on the *y* axis; *boxes* mark cells in the sub-G_0/G_1 (*yellow*), G_0/G_1 (*blue*), S (*green*), and G_2/M (*magenta*) phases of the cell cycle. Percentages of cells present in sub-G_0/G_1 and S populations are indicated. *Alexa488*, Alexa Fluor 488. *E*, immunofluorescence of BLM foci formation in nuclei after HU (0.5 mM) treatment of MEFs and recovery for the indicated times. Images compiled from different regions of a single micrograph are juxtaposed and separated by a *white line*. *F*, quantitation of *E*; data (mean ± S.E. $n = 200$) are compiled from two experiments. *G*, quantitation of chromosomal lesions in metaphase spreads from MEFs after treatment with mitomycin C (12 h, 300 nM) (mean ± S.E. $n = 28$). *H*, BLM foci formation in nuclei after HU (12 h, 0.5 mM) treatment of wild type MEFs transduced with lentivirus encoding either nontargeting shRNA or shRNA directed against IP6K2, and recovery for the indicated times. *I*, quantitation of *H*; data (mean ± S.E. $n = 200$) are compiled from two experiments. *p* values are from a two-tailed Student's *t* test (**, $p \leq 0.01$, ***, $p \leq 0.001$).

lapping roles in maintaining genome integrity. Such experiments are currently underway.

At a mechanistic level, we observe that inositol pyrophosphate synthesis by IP6K1 is essential for the completion of HR, as evidenced by the lack of repair in IP6K1$^{-/-}$ MEFs expressing catalytically inactive IP6K1. Inositol pyrophosphates may regulate the later stages of HR by binding or pyrophosphorylating one or more proteins involved in these processes. We are currently examining these possibilities using radiolabeled IP_7 along with purified proteins in IP_7 binding and pyrophosphorylation assays. Interestingly, we have identified HR proteins that are potential targets of IP_7, based on the presence of acidic serine sequence motifs that define sites for serine pyrophosphorylation.

The reported nuclear localization of IP6K1 supports our observations regarding its critical role in DNA repair (7). Our work also contributes to the body of information available on nuclear roles of other higher inositol phosphates (4). Previous studies have demonstrated a role for IP_4 and IP_5 in chromatin remodeling (38, 39). IP_6 is involved in mRNA export (40–42) and DNA repair via nonhomologous end joining (43).

In summary, our data reveal a role for inositol pyrophosphates synthesized by IP6K1 in HR-mediated repair of DSBs in mammalian cells. Inositol pyrophosphates are not involved in cell cycle checkpoint activation or HR initiation, but participate in the successful completion of HR. The absence of IP6K1 renders cells more susceptible to DNA damage agents. Because many cancer therapeutic strategies involve DNA replication stress, which leads to DSBs (44), we speculate that inhibition of IP6K1 activity may be used to supplement chemotherapy. Further work is required to determine the effects of reducing IP6K1 activity on the outcome of cancer chemotherapeutics.

Acknowledgments—We thank R. Manorama and J. Leyton-Mange for generating inactive IP6K1; M. Bala, Deepti, J. P. Vallentyne, and Sudheer K. R. for technical assistance; G. Ramakrishna, R. Wadhwa, and S. Tyagi for reagents and cell lines; A. Saiardi, A. Resnick, R. Tirumalai, R. Kaur, and all Laboratory of Cell Signalling personnel for valuable feedback.

REFERENCES

1. Chakraborty, A., Kim, S., and Snyder, S. H. (2011) Inositol pyrophosphates as mammalian cell signals. *Sci. Signal.* **4,** re1
2. Azevedo, C., Szijgyarto, Z., and Saiardi, A. (2011) The signaling role of inositol hexakisphosphate kinases (IP_6Ks). *Adv. Enzyme Regul.* **51,** 74–82
3. Shears, S. B., Gokhale, N. A., Wang, H., and Zaremba, A. (2011) Diphosphoinositol polyphosphates: what are the mechanisms? *Adv. Enzyme Regul.* **51,** 13–25
4. Monserrate, J. P., and York, J. D. (2010) Inositol phosphate synthesis and the nuclear processes they affect. *Curr. Opin. Cell Biol.* **22,** 365–373
5. Wang, H., Falck, J. R., Hall, T. M., and Shears, S. B. (2012) Structural basis for an inositol pyrophosphate kinase surmounting phosphate crowding. *Nat. Chem. Biol.* **8,** 111–116
6. Saiardi, A., Erdjument-Bromage, H., Snowman, A. M., Tempst, P., and Snyder, S. H. (1999) Synthesis of diphosphoinositol pentakisphosphate by a newly identified family of higher inositol polyphosphate kinases. *Curr. Biol.* **9,** 1323–1326
7. Saiardi, A., Nagata, E., Luo, H. R., Snowman, A. M., and Snyder, S. H. (2001) Identification and characterization of a novel inositol hexakisphosphate kinase. *J. Biol. Chem.* **276,** 39179–39185
8. Lee, Y. S., Huang, K., Quiocho, F. A., and O'Shea, E. K. (2008) Molecular basis of cyclin-CDK-CKI regulation by reversible binding of an inositol pyrophosphate. *Nat. Chem. Biol.* **4,** 25–32
9. Chakraborty, A., Koldobskiy, M. A., Bello, N. T., Maxwell, M., Potter, J. J., Juluri, K. R., Maag, D., Kim, S., Huang, A. S., Dailey, M. J., Saleh, M., Snowman, A. M., Moran, T. H., Mezey, E., and Snyder, S. H. (2010) Inositol pyrophosphates inhibit Akt signaling, thereby regulating insulin sensitivity and weight gain. *Cell* **143,** 897–910
10. Prasad, A., Jia, Y., Chakraborty, A., Li, Y., Jain, S. K., Zhong, J., Roy, S. G., Loison, F., Mondal, S., Sakai, J., Blanchard, C., Snyder, S. H., and Luo, H. R. (2011) Inositol hexakisphosphate kinase 1 regulates neutrophil function in innate immunity by inhibiting phosphatidylinositol-(3,4,5)-trisphosphate signaling. *Nat. Immunol.* **12,** 752–760
11. Saiardi, A., Bhandari, R., Resnick, A. C., Snowman, A. M., and Snyder, S. H. (2004) Phosphorylation of proteins by inositol pyrophosphates. *Science* **306,** 2101–2105
12. Bhandari, R., Saiardi, A., Ahmadibeni, Y., Snowman, A. M., Resnick, A. C., Kristiansen, T. Z., Molina, H., Pandey, A., Werner, J. K., Jr., Juluri, K. R., Xu, Y., Prestwich, G. D., Parang, K., and Snyder, S. H. (2007) Protein pyrophosphorylation by inositol pyrophosphates is a posttranslational event. *Proc. Natl. Acad. Sci. U.S.A.* **104,** 15305–15310
13. Azevedo, C., Burton, A., Ruiz-Mateos, E., Marsh, M., and Saiardi, A. (2009) Inositol pyrophosphate mediated pyrophosphorylation of AP3B1 regulates HIV-1 Gag release. *Proc. Natl. Acad. Sci. U.S.A.* **106,** 21161–21166
14. Szijgyarto, Z., Garedew, A., Azevedo, C., and Saiardi, A. (2011) Influence of inositol pyrophosphates on cellular energy dynamics. *Science* **334,** 802–805
15. Saiardi, A., Resnick, A. C., Snowman, A. M., Wendland, B., and Snyder, S. H. (2005) Inositol pyrophosphates regulate cell death and telomere length through phosphoinositide 3-kinase-related protein kinases. *Proc. Natl. Acad. Sci. U.S.A.* **102,** 1911–1914
16. York, S. J., Armbruster, B. N., Greenwell, P., Petes, T. D., and York, J. D. (2005) Inositol diphosphate signaling regulates telomere length. *J. Biol. Chem.* **280,** 4264–4269
17. Huang, K. N., and Symington, L. S. (1995) Suppressors of a *Saccharomyces cerevisiae pkc1* mutation identify alleles of the phosphatase gene *PTC1* and of a novel gene encoding a putative basic leucine zipper protein. *Genetics* **141,** 1275–1285
18. Luo, H. R., Saiardi, A., Yu, H., Nagata, E., Ye, K., and Snyder, S. H. (2002) Inositol pyrophosphates are required for DNA hyperrecombination in protein kinase c1 mutant yeast. *Biochemistry* **41,** 2509–2515
19. Li, X., and Heyer, W. D. (2008) Homologous recombination in DNA repair and DNA damage tolerance. *Cell Res.* **18,** 99–113
20. Hartwell, L. (1992) Defects in a cell cycle checkpoint may be responsible for the genomic instability of cancer cells. *Cell* **71,** 543–546
21. Bhandari, R., Juluri, K. R., Resnick, A. C., and Snyder, S. H. (2008) Gene deletion of inositol hexakisphosphate kinase 1 reveals inositol pyrophosphate regulation of insulin secretion, growth, and spermiogenesis. *Proc. Natl. Acad. Sci. U.S.A.* **105,** 2349–2353
22. Akagi, T., Sasai, K., and Hanafusa, H. (2003) Refractory nature of normal human diploid fibroblasts with respect to oncogene-mediated transformation. *Proc. Natl. Acad. Sci. U.S.A.* **100,** 13567–13572
23. Sengupta, S., Linke, S. P., Pedeux, R., Yang, Q., Farnsworth, J., Garfield, S. H., Valerie, K., Shay, J. W., Ellis, N. A., Wasylyk, B., and Harris, C. C. (2003) BLM helicase-dependent transport of p53 to sites of stalled DNA replication forks modulates homologous recombination. *EMBO J.* **22,** 1210–1222
24. Saintigny, Y., Delacôte, F., Varès, G., Petitot, F., Lambert, S., Averbeck, D., and Lopez, B. S. (2001) Characterization of homologous recombination induced by replication inhibition in mammalian cells. *EMBO J.* **20,** 3861–3870
25. Ward, I. M., and Chen, J. (2001) Histone H2AX is phosphorylated in an ATR-dependent manner in response to replicational stress. *J. Biol. Chem.* **276,** 47759–47762
26. Paull, T. T., Rogakou, E. P., Yamazaki, V., Kirchgessner, C. U., Gellert, M., and Bonner, W. M. (2000) A critical role for histone H2AX in recruitment of repair factors to nuclear foci after DNA damage. *Curr. Biol.* **10,**

886–895
27. Tikoo, S., and Sengupta, S. (2010) Time to bloom. *Genome Integr.* **1,** 14
28. Hendzel, M. J., Wei, Y., Mancini, M. A., Van Hooser, A., Ranalli, T., Brinkley, B. R., Bazett-Jones, D. P., and Allis, C. D. (1997) Mitosis-specific phosphorylation of histone H3 initiates primarily within pericentromeric heterochromatin during G_2 and spreads in an ordered fashion coincident with mitotic chromosome condensation. *Chromosoma* **106,** 348–360
29. Scully, R., Puget, N., and Vlasakova, K. (2000) DNA polymerase stalling, sister chromatid recombination, and the *BRCA* genes. *Oncogene* **19,** 6176–6183
30. Zinkel, S. S., Hurov, K. E., Ong, C., Abtahi, F. M., Gross, A., and Korsmeyer, S. J. (2005) A role for proapoptotic BID in the DNA-damage response. *Cell* **122,** 579–591
31. Luo, H. R., Saiardi, A., Nagata, E., Ye, K., Yu, H., Jung, T. S., Luo, X., Jain, S., Sawa, A., and Snyder, S. H. (2001) GRAB: a physiologic guanine nucleotide exchange factor for Rab3A, which interacts with inositol hexakisphosphate kinase. *Neuron* **31,** 439–451
32. Morrison, B. H., Haney, R., Lamarre, E., Drazba, J., Prestwich, G. D., and Lindner, D. J. (2009) Gene deletion of inositol hexakisphosphate kinase 2 predisposes to aerodigestive tract carcinoma. *Oncogene* **28,** 2383–2392
33. Moynahan, M. E., and Jasin, M. (2010) Mitotic homologous recombination maintains genomic stability and suppresses tumorigenesis. *Nat. Rev. Mol. Cell Biol.* **11,** 196–207
34. Yoshihara, T., Ishida, M., Kinomura, A., Katsura, M., Tsuruga, T., Tashiro, S., Asahara, T., and Miyagawa, K. (2004) XRCC3 deficiency results in a defect in recombination and increased endoreduplication in human cells. *EMBO J.* **23,** 670–680
35. Onnebo, S. M., and Saiardi, A. (2009) Inositol pyrophosphates modulate hydrogen peroxide signalling. *Biochem. J.* **423,** 109–118
36. Illies, C., Gromada, J., Fiume, R., Leibiger, B., Yu, J., Juhl, K., Yang, S.-N., Barma, D. K., Falck, J. R., Saiardi, A., Barker, C. J., and Berggren, P.-O. (2007) Requirement of inositol pyrophosphates for full exocytotic capacity in pancreatic cells. *Science* **318,** 1299–1302
37. Nagata, E., Luo, H. R., Saiardi, A., Bae, B. I., Suzuki, N., and Snyder, S. H. (2005) Inositol hexakisphosphate kinase-2, a physiologic mediator of cell death. *J. Biol. Chem.* **280,** 1634–1640
38. Steger, D. J., Haswell, E. S., Miller, A. L., Wente, S. R., and O'Shea, E. K. (2003) Regulation of chromatin remodeling by inositol polyphosphates. *Science* **299,** 114–116
39. Shen, X., Xiao, H., Ranallo, R., Wu, W. H., and Wu, C. (2003) Modulation of ATP-dependent chromatin-remodeling complexes by inositol polyphosphates. *Science* **299,** 112–114
40. York, J. D., Odom, A. R., Murphy, R., Ives, E. B., and Wente, S. R. (1999) A phospholipase C-dependent inositol polyphosphate kinase pathway required for efficient messenger RNA export. *Science* **285,** 96–100
41. Alcázar-Román, A. R., Tran, E. J., Guo, S., and Wente, S. R. (2006) Inositol hexakisphosphate and Gle1 activate the DEAD-box protein Dbp5 for nuclear mRNA export. *Nat. Cell Biol.* **8,** 711–716
42. Weirich, C. S., Erzberger, J. P., Flick, J. S., Berger, J. M., Thorner, J., and Weis, K. (2006) Activation of the DExD/H-box protein Dbp5 by the nuclear-pore protein Gle1 and its coactivator InsP6 is required for mRNA export. *Nat. Cell Biol.* **8,** 668–676
43. Hanakahi, L. A., Bartlet-Jones, M., Chappell, C., Pappin, D., and West, S. C. (2000) Binding of inositol phosphate to DNA-PK and stimulation of double-strand break repair. *Cell* **102,** 721–729
44. Allen, C., Ashley, A. K., Hromas, R., and Nickoloff, J. A. (2011) More forks on the road to replication stress recovery. *J. Mol. Cell Biol.* **3,** 4–12

DNA and Chromosomes:

Inositol Pyrophosphate Synthesis by Inositol Hexakisphosphate Kinase 1 Is Required for Homologous Recombination Repair

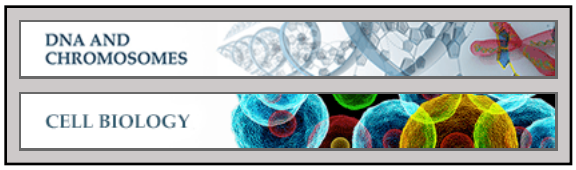

Rathan S. Jadav, Manasa V. L. Chanduri, Sagar Sengupta and Rashna Bhandari

J. Biol. Chem. 2013, 288:3312-3321.
doi: 10.1074/jbc.M112.396556 originally published online December 19, 2012